Integrated flexible-grid WDM transmitter using an optical frequency comb in microring modulators

Yelong Xu, Jiachuan Lin, Raphaël Dubé-Demers, Sophie LaRochelle, Leslie A. Rusch, and Wei Shi

OSA Optics Letters, (Volume 43, Issue 7) (2018)

Doi: 10.1364/OL.43.001554

https://www.osapublishing.org/ol/abstract.cfm?uri=ol-43-7-1554

National Science and Engineering Research Council of Canada (NSERC) Funding: CRDPJ499664

Integrated flexible-grid WDM transmitter using an optical frequency comb in microring modulators

YELONG XU, JIACHUAN LIN, RAPHAËL DUBÉ-DEMERS, SOPHIE LAROCHELLE, LESLIE RUSCH, AND WEI SHI

Department of Electrical and Computer Engineering, Centre d'optique photonique et laser (COPL), Université Laval, Québec, Canada

**Corresponding author: wei.shi@gel.ulaval.ca*

Advanced optical interconnects require high-speed links, which can be achieved by combining high channel rates with wavelength-division multiplexing (WDM). We report a multi-channel transmitter using cascaded microring modulators (MRMs) in silicon photonics. One MRM works as a flexible-grid optical comb generator, while the others work as channel modulators. With a single-wavelength laser input, we achieve flexible channel spacing (up to 25 GHz) with a tone-to-noise ratio (TNR) above 54 dB, all at low power consumption (less than 4.6 mW). We examine experimentally multi-channel transmission modulating data onto adjacent comb lines without significant signal crosstalk. This single-laser, flexible-grid WDM transmitter is a scalable solution: more comb lines can be obtained using uncoupled MRMs in series. This is the first demonstration of monolithic integration of a comb generator and multi-channel modulators for ultra-compact, power-efficient WDM photonic interconnects.

OCIS codes: *(230.4110) Modulators; (130.0130) Integrated optics; (060.4510) Optical communications; (230.5750) Resonators.*

Driven by the demand for ultrahigh-speed data transmission in computing systems and data centers, there is an urgent need for faster optical interconnects at low cost and low power. Leveraging the mature complementary metal-oxide semiconductor (CMOS) fabrication processes, silicon photonics (SiP) has quickly emerged as a disruptive large-scale photonic integration technology to respond to this need. Among SiP devices, the silicon microring modulator (MRM) [1-2] is a key component due to many desirable features such as compactness and low power consumption. MRM filtering ability makes cascaded MRMs accompanied with a multi-wavelength laser source a promising method of creating multiple independently modulated data streams at different wavelengths for short-reach wavelength-division multiplexing (WDM) links [3].

A multi-wavelength WDM laser source can be generated by either a laser array [4] or a comb source [5-10]. Compared to laser arrays, optical frequency combs require fewer optical inputs and are more compact, key features for an integrated solution. Alone among comb source approaches, a modulator-based comb source has flexible comb spacing and low power consumption. The flexible comb spacing could alleviate wasted spectrum in traditional WDM networks (due to guard bands in the fixed grid), and also provide the capability to flexibly adapt the spectrum allocation to traffic demand [11]. A modulator-based comb source is generated by sinusoidal modulation of a continuous-wave laser using an appropriate arrangement of electro-optic phase shifters; the comb spacing can be flexibly defined by the modulation frequency.

Generation of optical frequency combs using modulators has been realized using conventional $LiNO_3$ modulators [8], silicon-organic hybrid modulators [9] and InP photonic integrated circuits [10]. However, all these materials are not compatible with standard CMOS processes. This has hindered the co-integration of comb sources with silicon photonic transmitters. Monolithic integration of a comb generator with transmitters on silicon has not been demonstrated, despite its clear advantage.

In this letter, we report the operation of cascaded MRMs as a flexible-grid WDM silicon photonic transmitter. With a single-wavelength laser input, the proposed transmitter uses one or more MRMs for comb generation, and the rest of the MRMs in the cascade for data modulation. We show that high-quality comb lines (WDM carriers) can be generated with flexible channel spacing; they can support simultaneous multi-channel data transmission without significant signal degradation. To the best of our knowledge, this result represents the first single-laser flexible-grid WDM silicon photonic transmitter, which has not only a small footprint, but also low power consumption.

Figure 1(a) shows the principle of operation of the flexible-grid WDM transmitter. Cascaded MRMs are coupled in series to a single bus waveguide in an all-pass configuration. The first MRM (MRM0) works as a comb generator, where an RF synthesizer provides sinusoidal modulation at a defined frequency F_0. The comb line spacing is flexibly tuned by varying modulation frequency. The presence of the microring cavity with the phase shifter enhances the phase modulation near the resonance; multiple passages of light through the device facilitates the interaction between optical

National Science and Engineering Research Council of Canada (NSERC) Funding: CRDPJ499664

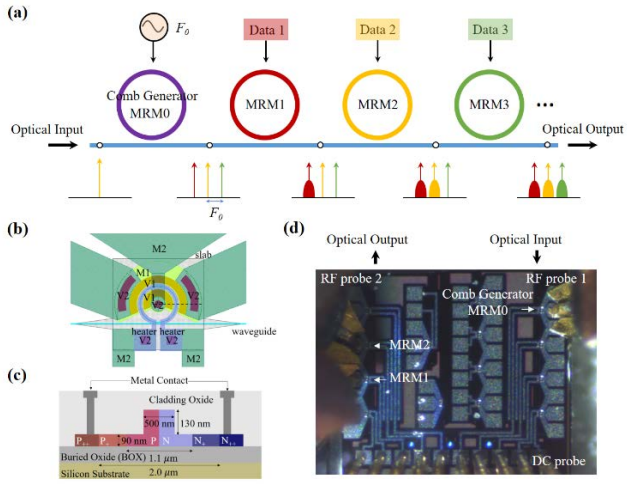

Fig. 1 (a) Schematic of a flexible-grid WDM silicon photonic transmitter based on cascaded microring modulators. (b) Layout of the MRM showing the metal layers (M1, M2), vias (V1, V2) and heaters. (c) Cross section of the p-n junction of the modulator showing relevant dimensions. (d) Photograph of the fabricated device connected with RF and DC probes.

and RF field [12,13]. When the microring cavity is operated near the critical coupling condition, the phase change induced by modulation near the resonance is very steep. This enables efficient phase modulation with a low driving power. Here MRM0 should ideally be operated near the critical coupling condition that can be achieved via careful process calibration and fine tuning of the bias voltage. We study three comb lines generated by the efficient phase modulation near resonance. These comb lines include the center frequency and the first-order optical sidebands. As the MRM0 also performs as a notch filter, by carefully tuning its resonance with respect to the laser center frequency, the power of the center frequency can be suppressed to some extent. In this way, we can make the three comb lines flat, desirable in WDM applications. MRM1, MRM2 and MRM3 are aligned to the three flexible-grid comb lines and modulated simultaneously by three independent RF signals. Thus, MRM0 and MRM1,2,3 make up the flexible-grid WDM transmitter system. However, due to a limited number of RF probes, we only modulated two adjacent channels in our proof-of-concept experiment.

Figure 1(b), (c), (d) give the layout, the cross section and photograph of our devices. All the MRMs are identical and were designed using the model found in [14]. Each MRM has a radius of 10 μm and a coupling gap of 315 nm. They make use of the plasma dispersion effect through carrier depletion in a lateral p-n junction. The p-n junction for intracavity modulation spans roughly 70% of the circumference, whereas the metal-based heater for wavelength tuning spans roughly 95% of the circumference, as shown in the partial mask layout of Fig. 1(b). The cross section of the waveguide and p-n junction is shown in Fig. 1(c). The silicon waveguide has a thickness of 220 nm; a 90-nm-thick slab is used for electrical connections. The device was fabricated in a multi-project-wafer run at IME A*STAR, Singapore. Fig. 1(d) shows the photograph of the fabricated device connected with RF and DC probes. Light is input and output through two etched surface grating couplers (SGCs) for transverse-electric polarized light. The SGCs are placed at the edge of the chip; they are not visible in the

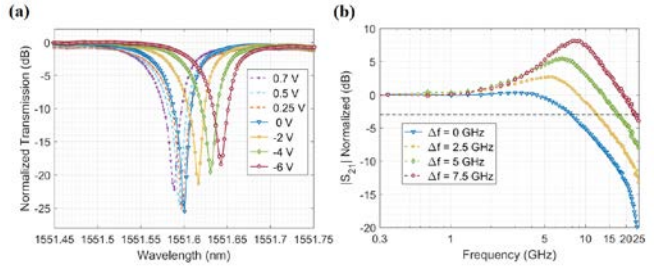

Fig. 2 (a) Measured power transmission spectra in the vicinity of the resonance of MRM0. (b) Measured EO scattering parameter S_{21} of MRM0 as a function of the frequency. S_{21} values are measured for various detuning frequencies and normalized at 300 MHz. The dashed horizontal line indicates the −3 dB level.

photograph. The RF pads on the left and right sides are used to apply RF signals for modulation on the MRM via RF probes. The DC pads at the bottom are used to apply DC voltages for thermal tuning on the heaters via DC probe.

The measured optical transmission spectra of MRM0 for various bias voltages are presented in Fig. 2(a). The figure shows that the resonance depth of around 26 dB at zero bias decreases as the reverse potential increases, indicating an overcoupling condition in reverse bias. The resonance depth decreases as the forward potential increases, indicating an undercoupling condition in forward bias. This behavior confirms that MRM0 is at near critical coupling at zero bias. The resonance shift as a function of reverse bias voltage shows an efficiency of about 1 GHz/V. In addition, the measured free spectral range (FSR) is 9.85 nm and the quality factor at equilibrium is 27,000.

The electro-optic (EO) S_{21} responses of MRM0 under zero bias are measured and shown in Fig. 2(b). Measurements are made for various frequency detuning, Δf, defined as the frequency of the optical input minus the resonant frequency of the cavity. The measured EO S_{21} responses at different detuning frequencies have peaks at high frequencies, while the response at the resonance is almost flat. This peaking and enhancement effect of the 3-dB EO bandwidth is due to the light at larger frequency detuning being is more easily released from the microring resonator, and thus having a shorter photon life-time [15,16]. The measured 3-dB EO bandwidth of MRM0 is close to 25 GHz at 7.5 GHz detuning.

A schematic of the experimental setup for optical comb generation, data transmission and characterization is shown in Fig.3. The sinusoidal signal from the RF synthesizer is amplified with a 50 GHz RF amplifier to 5 V_{pp}. The electrical signal is then sent via a microprobe with 50 GHz RF bandwidth, 50 Ω terminated GSG (Ground-Signal) configuration. The microprobe is applied to the RF pads of MRM0. We use a polarization maintaining fiber, fed with a tunable laser as the optical input, to ensure an optimal coupling with the SGCs. The measured fiber-to-fiber insertion loss (IL) of the SOI chip is approximately 13 dB where 10.5 dB of the IL is due to the SGCs. We use an optical isolator at the output of the chip, followed by an erbium-doped fiber amplifier (EDFA) to boost

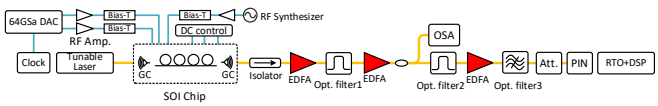

Fig. 3. Experimental setup for optical comb generation, data transmission and characterization.

National Science and Engineering Research Council of Canada (NSERC) Funding: CRDPJ499664

the signal, with amplified spontaneous emission (ASE) suppressed using a tunable optical bandpass filter (optical filter 1). The generated comb spectra are measured by optical spectrum analyzer (OSA) which has a resolution of 100 MHz.

To carry out data transmission of the on-chip comb, we tune DC voltages contolling MRM heaters to align MRM1 and MRM2 with two adjacent comb lines. We then use a GSGSG configured, 50 Ω terminated, 50 GHz microprobe to feed the electrical signals on-chip. The two digitally pulse-shaped 10 Gb/s on–off keying (OOK) electric signals of a pseudo-random binary sequence (PRBS) of $2^{19} - 1$ and a PRBS of $2^{20} - 1$ are generated by 64 GSamples/s digital-to-analog converter (DAC). Each of the electric signals is amplified with a 50 GHz RF amplifier to 5 V_{pp} and bias-coupled through a 70 GHz bias tee.

For the BER experiment, two additional stages of amplification are required to boost the signal; the EDFAs provide gain, while the optical filters (2 and 3) improve OSNR by suppressing out of band ASE noise. A variable optical attenuator controls the received power. A 60 GHz photodetector is used for optical-to-electrical conversion. The electrical signal is captured by a real-time oscilloscope (RTO) with 30 GHz analog bandwidth at 80 GSamples/s. Finally, BER is calculated offline by comparing the received data with the transmitted PRBS.

By carefully optimizing the voltage on the heater of MRM0 at zero bias three comb lines with 20 GHz channel spacing are generated as shown in Fig. 4(a). A TNR of 56 dB and flatness (intensity variation) of 2 dB is achieved. Since the comb frequency spacing is determined by the modulation frequency of the RF synthesizer, it can easily be adjusted by tuning the input RF frequency. By tuning the RF frequency to 25 GHz, the three comb lines are 25 GHz apart, as shown in Fig. 4(b). In this case, we have about 4 dB intensity variation and 54 dB TNR at the optimized operating condition.

To investigate the quality of the generated optical comb lines for WDM transmission, we tune the voltage on the heater to align MRM1 with one of the three channels: channel 1 (1554 nm), channel 2 (1554.16 nm) or channel 3 (1553.84 nm) shown in Fig. 5(a). The measured BER for MRM1 tuned to each channel is shown in Fig.5(b). The horizontal line indicates the $3.8 \cdot 10^{-3}$ pre-forward error correction code (FEC) threshold (for a 6.7% overhead) for error-free transmission, i.e., the post-FEC BER will be below 10^{-15} [17]. The BER of each channel stays below the FEC threshold when the received optical power reaches around -8.8 dBm for 20 GHz channel spacing. A small power penalty of around 0.2 dB between different channels reflects the good flatness of the optical comb.

To demonstrate concurrent multi-channel data transmission, we tune DC voltages to align MRM1 and MRM2 concurrently with two adjacent channel grids at 1554 nm and 1554.16 nm,

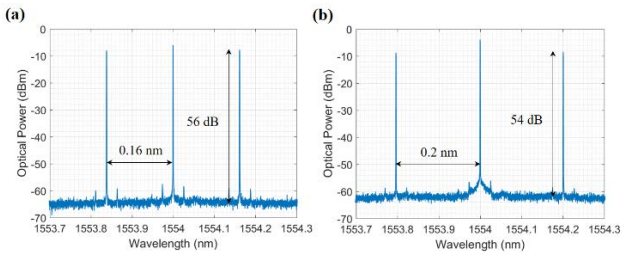

Fig. 4. (a) Spectrum of three comb lines generated by MRM0 at 20 GHz (0.16 nm) channel spacing. (b) Spectrum of three comb lines generated by MRM0 at 25 GHz (0.2 nm) channel spacing.

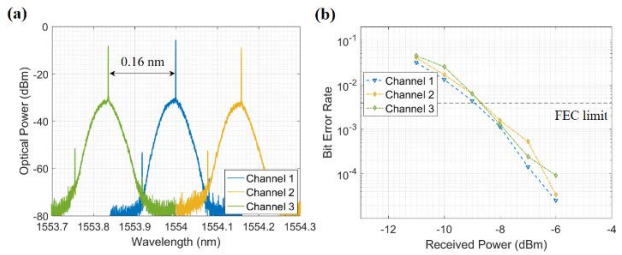

Fig. 5. (a) Spectrum after data transmission when MRM1 is aligned at 20 GHz comb line with channel 1 (1554 nm), channel 2 (1554.16 nm) and channel 3 (1553.84 nm), respectively. (b) BER measurements for MRM1 aligned at each comb line.

respectively. Fig. 6(a) illustrates the optical spectrum of simultaneously modulation of two adjacent channels with 20GHz spacing by MRM1 and MRM2. Since each of the two pulse-shaped electrical signals occupies a spectrum width of 20 GHz, the two modulated optical signals sit just side-by-side. Despite the absence of a guard band, there is no obvious crosstalk. Similarly, while the frequency of the RF synthesizer is 25 GHz, MRM1 and MRM2 are aligned with two adjacent channel grids at 1554 nm and 1554.2 nm, respectively. As shown in Fig. 6(b), there is about 5 GHz guard band at this comb separation, and there is no significant wavelength crosstalk between the adjacent channels. Fig. 6(c) and Fig. 6(d) present measured dependency of the BERs with received optical power at 10 Gb/s of different channels with 20 GHz and 25 GHz channel spacing, respectively. The counted BER is below the FEC threshold when the received optical power reaches around -8.6 dBm and -8 dBm for 20 GHz and 25 GHz channel spacing, respectively. Comparing to single channel transmission at 20 GHz channel spacing, there is only about 0.2 dB power penalty which indicates a very stable frequency spacing of the comb. The corresponding optical eye diagrams of different channels for 20 GHz and 25 GHz spacing with received power of 0 dBm are shown

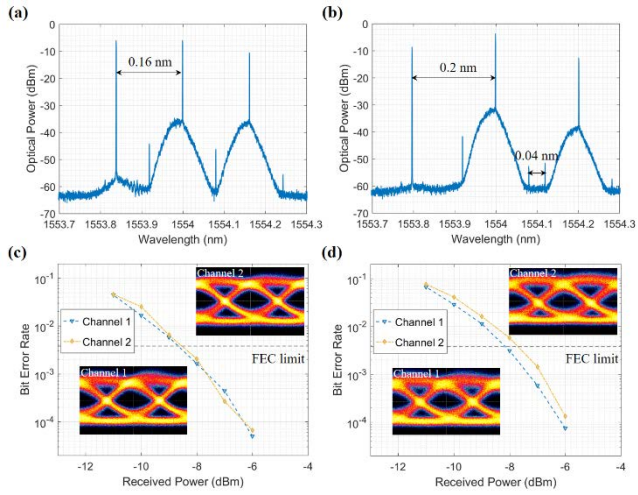

Fig. 6. (a), (b) Spectrum after simultaneous data transmission of channel 1 and 2 at adjacent 20 GHz (0.16 nm) and 25 GHz (0.2 nm) channel grid. (c) (d) BER measurements. Lower left and upper right insets are measured optical eye diagrams at 10 Gb/s for channel 1 and channel 2, respectively. The received power in all eye diagrams is around 0 dBm.

National Science and Engineering Research Council of Canada (NSERC) Funding: CRDPJ499664

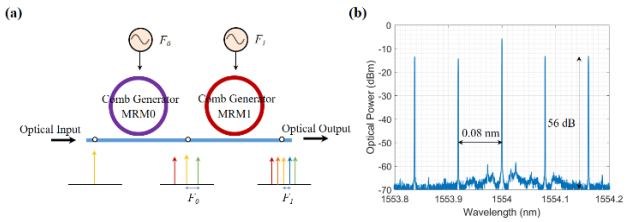

Fig. 7. (a) Schematic of cascaded comb generators based on MRMs. The RF frequencies on MRM0 and MRM1 are F_0 = 20 GHz and F_1 = 10 GHz, respectively. (b) Spectrum of five comb lines at 10 GHz (0.08 nm) channel spacing.

in the inset of Fig. 6(c) and Fig. 6(d), respectively. The BER below FEC threshold accompanied by clear optical eye diagrams of MRM1 and MRM2 at different channel spacings prove the feasibility of this flexible-grid WDM transmitter.

This on-chip flexible-grid optical frequency comb is scalable: more comb lines can be obtained by using uncoupled MRMs in series for comb generation. For example, we used the same cascaded MRMs to produce 5 comb lines by using two MRMs for comb generation as shown in Fig. 7(a). Here we take MRM0 and MRM1 as flexible-grid comb generators. The RF driving frequency on MRM0 is F_0 = 20 GHz while RF frequency on MRM1 is F_1 = 10 GHz. By carefully optimizing voltages on the heaters of MRM0 and MRM1, as shown in Fig. 7(b), five comb lines with 10 GHz channel spacing are generated at the highest TNR which is better than 56 dB (up to 64 dB). It is worth mentioning that the flatness of the comb can be further improved by integrating an optical filter to suppress the center frequency. The scalable flexible-grid optical frequency comb can also be synthesized by superposition of different frequencies in the electric domain. Five highly uniform frequency tones (variation less than 0.7 dB) with a 10 GHz spacing was recently demonstrated in a single MRM by using a dual frequency electrical input at 10 GHz and 20 GHz [18].

The advantage of the phase modulator being inside the microring cavity for comb generation and data transmission is low power consumption. Here we give an estimation of the power consumed for comb generation which is mainly from charging the capacitor in the depletion region of the p-n junction [2]. The energy dissipated inside the modulator is given by product of $E=CV^2$, where C is the capacitance of the p-n junction and V is the driving voltage. The capacitance C here is calculated to be 7.3 fF using the model in reference [14]. The power for comb generation is about 3.7 mW and 4.6 mW for 20 GHz and 25 GHz channel spacing, respectively. In fact, the driving voltage of the comb generator could be further reduced by increasing the modulation efficiency of the modulator [2]. We also give an estimation on the power of tuning the MRMs to match to given channel wavelengths. The efficiency of the heater is measured to be 3.1 mW/nm. The power for thermal tuning here is estimated to be 1.5 mW and 1.9 mW for 20 GHz and 25 GHz channel spacing, respectively.

We have demonstrated MRM enabled on-chip comb generation and also proven the concept of single-laser flexible-grid WDM silicon photonic transmitter. The generated combs lines have high TNR (above 54 dB) and channel spacing going up to 25 GHz at low power consumption (less than 4.6 mW). For concurrent multi-channel transmission examined at 20 GHz and 25 GHz channel spacings, two MRMs are aligned to adjacent channel grids and simultaneously transmitted 10 Gb/s OOK data with low crosstalk. Furthermore, this is a scalable solution by which more comb lines can be enabled by cascading more MRM based comb generators. The device performance could be further improved by designing MRMs with larger EO bandwidth, which means larger baud rate data could be allocated at each channel. The bit rate at each channel can be increased by employing advanced modulation formats such as pulse-amplitude modulation [2] to provide higher spectral efficiency within a given bandwidth. This work represents a promising direction towards compact and power-efficient flexible-grid WDM CMOS photonic interconnects.

Funding. Fonds de Recherche du Québec-Nature et Technologies (FRQNT) (2016-NC-190737); National Science and Engineering Research Council of Canada (NSERC) (CRDPJ499664); PROMPT Quebec grant (52_Rusch 2016.09); TELUS; Aeponyx.

Acknowledgment. The authors thank H. Sepehrian and N. Landry from COPL for technical support. We further acknowledge the contribution and technical support of CMC Microsystems.

REFERENCES

1. G. Li, A. V. Krishnamoorthy, I. Shubin, J. Yao, Y. Luo, H. Thacker, X. Zheng, K. Raj, and J. E. Cunningham, IEEE J. Sel. Top. Quantum Electron. **19**, 3401819 (2013).
2. R. Dubé-Demers, S. LaRochelle, and W. Shi, Optica. **3**, 622–627 (2016).
3. P. Dong, IEEE J. Sel. Top. Quantum Electron. **22**, 370–378 (2016).
4. X. Zheng, E. Chang, I. Shubin, G. Li, Y. Luo, J. Yao, H. Thacker, J.-H. Lee, J. Lexau, F. Liu,P. Amberg, K. Raj, R. Ho, J. E. Cunningham, and A. V. Krishnamoorthy, in *Optical Fiber Communication Conference (OFC)* (2013), paper PDP5C.9
5. C.-H. Chen, M.A. Seyedi, M. Fiorentino, D. Livshits, A. Gubenko, S. Mikhrin, V. Mikhrin, and R. Beausoleil, Opt. Express **23**, 21541–21548 (2015).
6. N. Eiselt, H. Griesser, M. Eiselt, W. Kaiser, S. Aramideh, J. J. V. Olmos, I. T. Monroy, and J. Elbers, in *Optical Fiber Communication Conference (OFC)* (2017), paper W4D.3.
7. J. Pfeie, V. Brasch, M. Lauermann, Y. Yu, D. Wegner, T. Herr, K. Hartinger, P. Schindler, J. Li, D. Hillerkuss, R. Schmogrow, C. Weimann, R. Holzwarth, W. Freude, J. Leuthold, T. J. Kippenberg, and C. Koos, Nat. Photon. **8**, 375-380 (2014).
8. R. Wu, V. R. Supradeepa, C. M. Long, D. E. Leaird, and A. M. Weiner, Opt. Lett. **35**, 3234-3236 (2010).
9. A. K. Mishra, R. Schmogrow, I. Tomkos, D. Hillerkuss, C. Koos, W. Freude, and J. Leuthold, IEEE Photon. Technol. Lett. **25**, 701-704 (2013).
10. R. Slavík, S. G. Farwell, M. J. Wale, and D. J. Richardson, IEEE Photon. Technol. Lett. **27**, 217-220 (2015).
11. I. Tomkos, S. Azodolmolky, J. Sole-Pareta, D. Careglio, and E. Palkopoulou, Proc. IEEE. **102**, 1317–1337 (2014).
12. J. Ye, L. S. Ma, T. Daly, and J. L. Hall, Opt. Lett. **22**, 301-303 (1997).
13. X. Wu, and H. K. Tsang. *in Conference on Lasers and Electro-Optics (CLEO)* (2017), paper SM4O-6.
14. R. Dubé-Demers, J. St-Yves, A. Bois, Q. Zhong, M. Caverley, Y. Wang, L. Chrostowski, S. LaRochelle, D. V. Plant, and W. Shi, J. Lightwave Technol. **33**, 4240–4252 (2015).
15. J. Müller, F. Merget, S. S. Azadeh, J. Hauck, S. R. García, B. Shen, and J. Witzens, Sci. Rep. **4**, 6310 (2014).
16. H. Yu, D. Ying, M. Pantouvaki, J. Van Campenhout, P. Absil, Y. Hao, J. Yang, and X. Jiang, Opt.Express. **22**, 15178–15189 (2014).
17. "Media access control parameters, physical layers, and management parameters for 40-Gb/s and 100-Gb/s operation," IEEE Std. 802.3ba (2010).
18. I. Demirtzioglou, C. Lacava, K. R. H. Bottrill, D. J. Thomson, G. T. Reed, D. J. Richardson, and P. Petropoulos, Opt. Express **26**, 790-796 (2018).

REFERENCES

1. G. Li, A. V. Krishnamoorthy, I. Shubin, J. Yao, Y. Luo, H. Thacker, X. Zheng, K. Raj, and J. E. Cunningham, "Ring resonator modulators in silicon for interchip photonic links," IEEE J. Sel. Top. Quantum Electron. **19**, 3401819 (2013).
2. R. Dubé-Demers, S. LaRochelle, and W. Shi, "Ultrafast pulse-amplitude modulation with a femtojoule silicon photonic modulator," Optica. **3**, 622–627 (2016).
3. P. Dong, "Silicon photonic integrated circuits for wavelength-division multiplexing applications," IEEE J. Sel. Top. Quantum Electron. **22**, 370–378 (2016).
4. X. Zheng, E. Chang, I. Shubin, G. Li, Y. Luo, J. Yao, H. Thacker, J.-H. Lee, J. Lexau, F. Liu,P. Amberg, K. Raj, R. Ho, J. E. Cunningham, and A. V. Krishnamoorthy, "A 33 mW 100 Gbps CMOS Silicon Photonic WDM Transmitter Using Off-Chip Laser Sources," in *Optical Fiber Communication Conference (OFC)* (2013), paper PDP5C.9
5. C.-H. Chen, M.A. Seyedi, M. Fiorentino, D. Livshits, A. Gubenko, S. Mikhrin, V. Mikhrin, and R. Beausoleil, "A comb laser-driven DWDM silicon photonic transmitter based on microring modulators," Opt. Express **23**, 21541–21548 (2015).
6. N. Eiselt, H. Griesser, M. Eiselt, W. Kaiser, S. Aramideh, J. J. V. Olmos, I. T. Monroy, and J. Elbers, ""Real-time 200 Gb/s (4x56.25 Gb/s) PAM-4 transmission over 80 km SSMF using quantum-dot laser and silicon ring-modulator," in *Optical Fiber Communication Conference (OFC)* (2017), paper W4D.3.
7. J. Pfeie, V. Brasch, M. Lauermann, Y. Yu, D. Wegner, T. Herr, K. Hartinger, P. Schindler, J. Li, D. Hillerkuss, R. Schmogrow, C. Weimann, R. Holzwarth, W. Freude, J. Leuthold, T. J. Kippenberg, and C. Koos, "Coherent terabit communications with microresonator Kerr frequency combs," Nat. Photon. **8**, 375-380 (2014).
8. R. Wu, V. R. Supradeepa, C. M. Long, D. E. Leaird, and A. M. Weiner, "Generation of very flat optical frequency combs from continuous-wave lasers using cascaded intensity and phase modulators driven by tailored radio frequency waveforms," Opt. Lett. **35**, 3234-3236 (2010).
9. A. K. Mishra, R. Schmogrow, I. Tomkos, D. Hillerkuss, C. Koos, W. Freude, and J. Leuthold, "Flexible RF-based comb generator," IEEE Photon. Technol. Lett. **25**, 701-704 (2013).
10. R. Slavík, S. G. Farwell, M. J. Wale, and D. J. Richardson, "Compact Optical comb generator using InP tunable laser and push-pull modulator," IEEE Photon. Technol. Lett. **27**, 217-220 (2015).
11. I. Tomkos, S. Azodolmolky, J. Sole-Pareta, D. Careglio, and E. Palkopoulou, "A tutorial on the flexible optical networking paradigm: state of the art, trends, and research challenges," Proc. IEEE. **102**, 1317–1337 (2014).
12. J. Ye, L. S. Ma, T. Daly, and J. L. Hall, "Highly selective terahertz optical frequency comb generator," Opt. Lett. **22**, 301-303 (1997).
13. X. Wu, and H. K. Tsang. "Flat-top frequency comb generation with silicon microring modulator and filter," *in Conference on Lasers and Electro-Optics (CLEO)* (2017), paper SM4O-6.
14. R. Dubé-Demers, J. St-Yves, A. Bois, Q. Zhong, M. Caverley, Y. Wang, L. Chrostowski, S. LaRochelle, D. V. Plant, and W. Shi, "Analytical modeling of silicon microring and microdisk modulators with electrical and optical dynamics," J. Lightwave Technol. **33**, 4240–4252 (2015).
15. J. Müller, F. Merget, S. S. Azadeh, J. Hauck, S. R. García, B. Shen, and J. Witzens, "Optical peaking enhancement in high-speed ring modulators," Sci. Rep. **4**, 6310 (2014).
16. H. Yu, D. Ying, M. Pantouvaki, J. Van Campenhout, P. Absil, Y. Hao, J. Yang, and X. Jiang, "Trade-off between optical modulation amplitude and modulation bandwidth of silicon micro-ring modulators," Opt.Express. **22**, 15178–15189 (2014).
17. "Media access control parameters, physical layers, and management parameters for 40-Gb/s and 100-Gb/s operation," IEEE Std. 802.3ba (2010).
18. I. Demirtzioglou, C. Lacava, K. R. H. Bottrill, D. J. Thomson, G. T. Reed, D. J. Richardson, and P. Petropoulos, "Frequency comb generation in a silicon ring resonator modulator," Opt. Express **26**, 790-796 (2018)

National Science and Engineering Research Council of Canada (NSERC) Funding: CRDPJ499664